

Calibration and validation of projection lithography focusing by fluorescence detection of latent photoacid images in chemically amplified resist

G. D. Feke^{a)} and R. D. Grober^{b)}

Department of Applied Physics, Yale University, New Haven, Connecticut 06520-8284

G. Pohlers and J. F. Cameron

Shipley Company, Microelectronic Materials Research and Development Laboratories, Marlborough, Massachusetts 01752

(Received 15 May 2001; accepted 5 November 2001)

We dope the commercial resist UVIII with the *pH* sensitive dye coumarin 6 (C6) to demonstrate a fluorescence microscopy technique for detecting latent photoacid images in exposed chemically amplified resist films. The spectroscopic properties of C6 in the resist matrix are investigated in order to select spectroscopic filters which optimize the fluorescence image contrast of exposed patterns. We apply this technique to focus calibration of a projection lithography system and show a significant correlation of the results to scanning electron microscope analysis of developed features. Hence, we demonstrate the utility of this technique as a fabrication line diagnostic for focus calibration and validation (i.e., proof of focus) prior to postexposure processing of the resist film.

© 2002 American Vacuum Society. [DOI: 10.1116/1.1431957]

I. INTRODUCTION

Chemically amplified resists (CARs)¹ are widely used by the semiconductor industry and continue to be developed in response to the increasingly demanding requirements of production lithography. In this class of resists the radiation pattern incident at the wafer is recorded by photogeneration of a catalyst, typically a strong Brønsted acid produced by the photolytic decomposition of a photoacid generator. The photoacid is thermally activated by a postexposure bake (PEB) to catalyze multiple chemical reactions in the resist matrix and thereby locally alter the dissolution rate, a process called chemical amplification. The resist is then developed with the spatially dependent dissolution rate defining the ultimate pattern. The success of the CAR scheme is due to the decoupling of the exposure and the resist chemistry, so that the photospeed is effectively enhanced by the amplification process during PEB.

Precise control of the spatial distribution of photoacid during lithographic processing is paramount for maximizing lithographic resolution and minimizing critical dimension variation. For example, in projection lithography systems, the aerial image must be well focused at the wafer to generate a photoacid image that reproduces the mask as faithfully as possible. Proper focusing requires frequent calibration of the wafer scan stage. Photoacid distribution is generally inferred from developed patterns. However, because developed patterns represent the convolution of each and every lithographic process, it is not possible to determine the photoacid distribution at each stage and hence unambiguously characterize individual processes. Furthermore, in many cases it may be desirable to inspect the outcome of a particular process before proceeding to the next (e.g., validating that the

exposure was indeed in proper focus before PEB and development).

Several recent reports have demonstrated techniques involving fluorescence microscopy of resist doped with a *pH* indicator dye to detect latent photoacid images prior to postexposure processing.²⁻⁶ We herein report the application of fluorescence detection of latent photoacid images to calibration of the best focus of a projection lithography system. This investigation demonstrates the potential of this technique as a fabrication line diagnostic (specifically with regard, but not limited, to focus validation), where the ability to characterize the exposure step without the need to proceed through PEB and development would be advantageous. We used the commercial, positive-tone resist UVIII (Shipley Co.) doped with the commercially available laser dye coumarin 6 (C6).⁷⁻⁹ Because a dye must have at least two prototropic forms with different spectroscopic properties to exhibit fluorescence contrast as a function of *pH*,¹⁰ the fluorescence contrast between the two prototropic populations is maximal if one prototropic form may be spectroscopically probed without interaction with the other form. By exploiting the spectroscopic properties of C6, we obtain fluorescence images with very high contrast. We furthermore compare fluorescence images with scanning electron microscope (SEM) images of cross sections of the corresponding developed features.

II. EXPERIMENT

Previous studies which have employed C6 as an acid sensor (in CARs or otherwise) have demonstrated that the absorption and fluorescence spectra of the dye undergo a redshift upon protonation.^{6,11-17} However, the positions and shapes of these spectra generally depend on the chemical composition of the host matrix. Therefore, absorption and fluorescence spectroscopy of the neutral (C6) and monoca-

^{a)}Present address: JDS Uniphase Corp., Windsor, CT 06095.

^{b)}Electronic mail: robert.grober@yale.edu

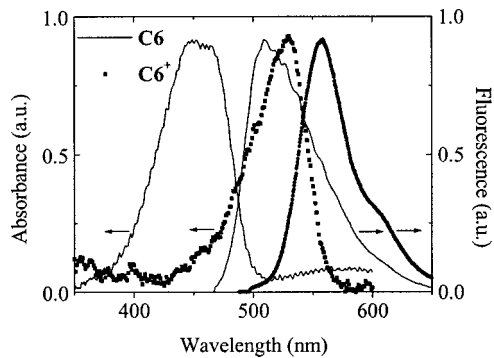


FIG. 1. Absorption and fluorescence spectra of C6 and C6⁺ in hydroxystyrene-co-t-butylacrylate.

tion (C6⁺) forms of the dye in UVIII were necessary in order to select the appropriate spectroscopic filters for fluorescence imaging.

Two formulations were prepared for spectroscopic analysis: A and B. Both were hydroxystyrene-co-t-butylacrylate (which is the UVIII resist matrix) doped with 1 wt % (vs solids content) C6. This high dye loading was necessary to provide a sufficient signal-to-noise ratio for absorption spectroscopy. A sulfonic acid was added to A until the formulation was observed by the naked eye to change color from green to orange. Hence, A contained C6⁺ whereas B contained C6. Each formulation was coated to a thickness of approximately 0.7 μm on a 1 in. quartz wafer and received a postapplication bake (PAB) at 130 $^{\circ}\text{C}$ for 60 s.

Absorption spectra were recorded using a Varian CARY 13 spectrophotometer. Fluorescence spectra were obtained from the identical samples as the absorption spectra using an apparatus based on a Triplemate monochromator. Sample A was excited with 488.0 nm light from an Ar-ion laser. Sample B was excited with 457.9 nm light. Both the absorption and the fluorescence spectra are shown in Fig. 1. The redshifts between the C6 and C6⁺ spectra are so large that little overlap exists between each pair.

The apparatus used for detecting latent photoacid images is based on a Zeiss Axioskop 50 microscope operated in epi-fluorescence mode. The spectroscopic filters were chosen to excite and detect the neutral population of the dye exclusively. Light from a 75 W xenon arc lamp is transmitted through a ground glass diffuser and a 457.9 ± 5 nm excitation filter, reflected by a 497 nm long pass dichroic beam splitter, and imaged onto the sample with a dry, 0.9 numerical aperture, 100 \times , infinity corrected microscope objective. Dry microscopy permits noncontact inspection, a necessity for a potential fabrication line diagnostic tool. The fluorescence is collected by the objective, transmitted through the dichroic beam splitter, a 500 nm long pass filter, a 515 ± 15 nm filter, and imaged onto a liquid nitrogen cooled 512×512 array $24 \times 24 \mu\text{m}$ pixel charge coupled device camera with 16 bit resolution by a combination of the microscope tube lens and a negative lens for additional magnification (a total of 492 \times). As can be seen in Fig. 1, the C6⁺ population is very weakly excited by light at 457.9 nm and is very weakly fluorescent between 500 and 530 nm. This choice of filters

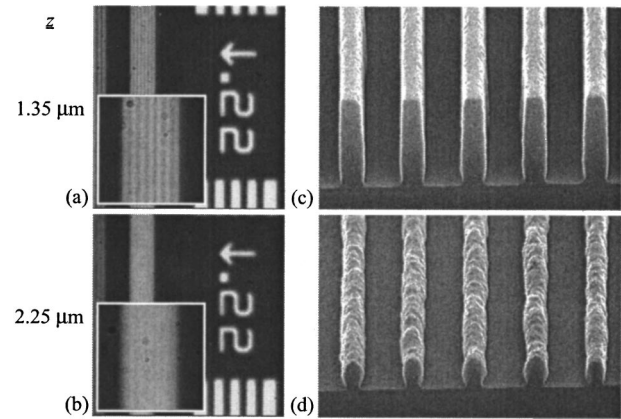


FIG. 2. (a) and (b) Fluorescence images of 0.22 μm lines at 0.44 μm pitch exposed at focus increment $z = 1.35$ and 2.25 μm , respectively. Insets show enlarged views of lines. (c) and (d) SEM images of the cross sections of the corresponding developed patterns.

therefore provides detection of C6 with very good contrast. Images were acquired using an integration time of 30 s in order to use a substantial fraction of the dynamic range of the camera (with the given excitation intensity). To achieve the best focus in the fluorescence microscope prior to image acquisition, the field diaphragm was closed partially and the sample stage was adjusted until the sharpest image of the field diaphragm edge was obtained.

A formulation of UVIII doped with 0.05 wt % C6 was prepared for focus calibration. Films were coated to a thickness of approximately 0.75 μm onto two 8 in. silicon wafers [each coated with an AR3 antireflective coating (Shipley Co.)] and received postapplication bakes at 130 $^{\circ}\text{C}$ for 60 s. Each of the wafers was exposed with a binary image mask consisting of various features using a GCA XLS 7800 projection lithography system. Since the field of view of the system is much smaller than the wafer area, the exposure was repeated at different positions on each of the wafers as the focus was ramped through a range of 2.4 μm in increments of 0.15 μm (a total of 17 samples). One of the wafers received a PEB at 130 $^{\circ}\text{C}$ for 90 s, developed using CD-26 (Shipley Co.), and underwent SEM analysis. The other wafer underwent fluorescence analysis directly after exposure.

The features chosen for focus calibration were an array of seven 0.22 μm lines at 0.44 μm pitch. Seventeen fluorescence images of these features were acquired, one for each focus increment (z). Two representative fluorescence images are shown in Fig. 2: (a) $z = 1.35 \mu\text{m}$ and (b) $z = 2.25 \mu\text{m}$ (where $z = 0$ is the beginning of the focus ramp). Because the spectroscopic filters were chosen to detect the neutral population of the dye, the regions of high intensity identify unexposed resist (i.e., regions of low acid concentration). The contrast between the lines and spaces in the fluorescence image at $z = 2.25 \mu\text{m}$ is significantly less than that at $z = 1.35 \mu\text{m}$ due to a weaker modulation of acid concentration, which indicates that the $z = 1.35 \mu\text{m}$ image is in better focus.

We note that if the spectroscopic filters had instead been chosen to excite and detect the monocation population of the

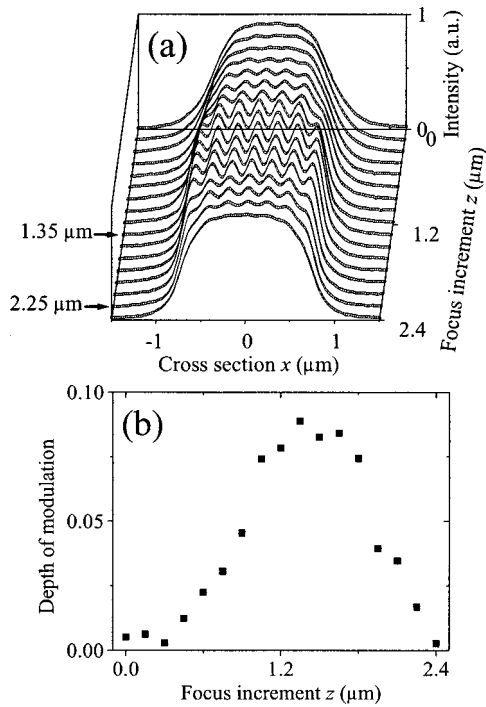


Fig. 3. (a) Cross sections of the fluorescence images as a function of focus increment z . (b) Depth of modulation [calculated from the cross sections in (a)] vs focus increment z .

dye exclusively, the reverse images would be produced. However, the optical resolution of the reverse images would be somewhat less because the fluorescence would be shifted to longer wavelengths.

SEM images of the cross sections of the developed features were acquired for each focus increment as well; those corresponding to Figs. 2(a) and 2(b) are shown in Figs. 2(c) and 2(d), respectively. Because the resist is positive-tone, the areas where the resist is present identify unexposed resist (i.e., regions without acid catalyzed dissolution enhancement, corresponding to opaque regions on the mask). Whereas the developed pattern at $z = 1.35 \mu\text{m}$ exhibits excellent quality, those at $z = 2.25 \mu\text{m}$ exhibit significant top-loss due to partial acid catalyzed deblocking of the polymer.

III. ANALYSIS

Fluorescence cross sections of each of the seventeen images are shown in Fig. 3(a). Arrows indicate the cross sections of the $z = 1.35 \mu\text{m}$ and $z = 2.25 \mu\text{m}$ images. The data for $-0.44 \mu\text{m} < x < 0.44 \mu\text{m}$ (where x is cross-sectional position) were fit with the function

$$a \sin(kx + \phi) + h + b, \quad (1)$$

where a (amplitude), k (spatial frequency), ϕ (phase), and h (offset) were free parameters, and b was a fixed parameter (the value of the baseline fluorescence in the exposed region). The depth of modulation

$$\text{DOM} \equiv a/h \quad (2)$$

was calculated for each of the cross sections and is shown as a function of z in Fig. 3(b). The data fall within two distinct

groups: whereas the DOM for $1.05 \mu\text{m} < z < 1.80 \mu\text{m}$ is larger than 0.074, the DOM for $z < 0.90 \mu\text{m}$ and $z > 1.95 \mu\text{m}$ is less than 0.046. The data therefore suggest that the wafer scan stage of the projection lithography system achieves best focus for $1.05 \mu\text{m} < z < 1.80 \mu\text{m}$, and that the depth of focus of the system is $1.80 \mu\text{m} - 1.05 \mu\text{m} = 0.75 \mu\text{m}$.

The focus latitude (FL) of a resist is defined as the focus range through which a given feature develops with a critical dimension (CD) within $\pm 10\%$ of the target CD and with less than 10% thickness loss. FL is a function of the properties of the resist as well as the optical depth of focus of the projection lithography system. The FL of this resist (for $0.22 \mu\text{m}$ lines) was calculated from the SEM images to be $0.90 \mu\text{m}$ (from $z = 0.90 \mu\text{m}$ to $z = 1.80 \mu\text{m}$). This result validates the fluorescence method. Therefore, the fluorescence method provides a robust calibration of the best focus of the wafer scan stage, as well as a means to validate whether an exposure was indeed in best focus before proceeding through PEB and development.

IV. SUMMARY

We have demonstrated a fluorescence technique for detection of latent photoacid images in chemically amplified resist. We have applied this technique to the focus calibration of the wafer scan stage of a projection lithography system and have shown that the fluorescence image may be used to validate the focus of exposed wafers prior to subsequent processing.

¹H. Ito, Proc. SPIE **3678**, 2 (1999).

²S. J. Bukofsky, G. D. Feke, Q. Wu, R. D. Grober, P. M. Dentinger, and J. W. Taylor, Appl. Phys. Lett. **73**, 408 (1998).

³P. L. Zhang, S. E. Webber, J. Mendenhall, J. D. Byers, and K. Chao, Proc. SPIE **3333**, 794 (1998).

⁴P. M. Dentinger, B. Lu, J. W. Taylor, S. J. Bukofsky, G. D. Feke, D. Hessman, and R. D. Grober, J. Vac. Sci. Technol. B **16**, 3767 (1998).

⁵B. Lu, J. W. Taylor, F. Cerrina, C. P. Soo, and A. J. Bourdillon, J. Vac. Sci. Technol. B **17**, 3345 (1999).

⁶C. Coenjarts, J. F. Cameron, N. Deschamps, D. Hambly, G. Pohlers, J. C. Scaiano, R. Sinta, S. Virdee, and A. Zampini, Proc. SPIE **3678**, 1062 (1999).

⁷M. S. A. Abdel-Mottaleb, R. O. Loutfy, and R. Lapouyade, J. Photochem. Photobiol., A **48**, 87 (1989).

⁸M. S. A. Abdel-Mottaleb, M. S. Antonious, M. M. Ali Abo, L. F. M. Ismail, B. A. El-Sayed, and A. M. K. Sherief, Proc. Indian Acad. Sci., Chem. Sci. **104**, 185 (1992).

⁹G. I. Jones, W. R. Jackson, and C. Choi, J. Phys. Chem. **89**, 294 (1985).

¹⁰J. Polster and H. Lachmann, *Spectrometric Titrations* (VCH, New York, 1989).

¹¹S. Corrent, P. Hahn, G. Pohlers, T. J. Connolly, J. C. Scaiano, V. Fornés, and H. Garcia, J. Phys. Chem. B **102**, 5852 (1998).

¹²G. Pohlers, J. C. Scaiano, and R. F. Sinta, Chem. Mater. **9**, 3222 (1997).

¹³J. F. Cameron, J. Mori, T. M. Zydowsky, D. Kang, R. F. Sinta, M. King, J. C. Scaiano, G. Pohlers, S. Virdee, and T. Connolly, Proc. SPIE **3333**, 680 (1998).

¹⁴E. Richter, S. Hien, and M. Sebald, J. Photopolym. Sci. Technol. **12**, 695 (1999).

¹⁵E. Richter, S. Hien, and M. Sebald, Microelectron. Eng. **53**, 479 (2000).

¹⁶C. Coenjarts, J. F. Cameron, G. Pohlers, J. C. Scaiano, and A. Zampini, J. Appl. Polym. Sci. **78**, 1897 (2000).

¹⁷G. D. Feke, R. D. Grober, G. Pohlers, K. Moore, and J. F. Cameron, Anal. Chem. **73**, 3472 (2001).